JOURNAL OF MATERIALS SCIENCE 10 (1975) 1381–1393

Time–temperature dependent fracture toughness of PMMA

Part 1

A. G. ATKINS, C. S. LEE, R. M. CADDELL
Department of Mechanical Engineering, University of Michigan, Ann Arbor, Michigan, USA

A toughness-biased Ree-Eyring relationship gives a good description of fracture toughness data of PMMA over a range of temperatures (283 to 353 K) and crack velocities (10^{-5} to 1 m sec^{-1}). Fracture toughness was measured by Gurney's sector method. The activation energy associated with the equation supports earlier work which suggests that, in the same temperature and velocity range, cracking in PMMA is controlled by craze growth, which is governed by secondary (β) molecular processes. Unstable cracking at moderate velocities (10^{-2} to 1 m sec^{-1}) seems to be produced by an isothermal/adiabatic transformation; an analysis for the onset of instability is given. At temperatures below 283 K, changes in toughness behaviour are seen, and below 243 K no stable cracking at all was obtained. A discussion is given of various methods of characterizing resistance to cracking, and methods of transforming $R(\dot{a}, T)$ and $K(\dot{a}, T)$ data are compared.

1. Introduction

A growing body of data demonstrates that the resistance to cracking in PMMA is both rate and temperature dependent. Early workers performed experiments where the crack speed (or strain rate) and temperature were not simultaneously varied, so that the data are uncoupled. For example, Benbow [1], Svenson [2], Berry [3], Broutman and McGarry [4], Key *et al.* [5] investigated the effect of temperature on resistance to cracking in PMMA (usually with cleavage specimens), where fixed testing machine cross-head speeds or fixed cross-head displacements were employed. Strain rate was not considered a significant variable, and average values of some crack resistance parameters were quoted for every temperature. Similarly, most early time-dependent crack resistance tests were performed at room temperature, using crack speed as a parameter to represent strain rate at the crack tip; see for example, Vincent and Gotham [6], Williams *et al.* [7] and Marshall *et al.* [8]. Experiments in which both rate and temperature have been simultaneously varied are those of Olear and Erdogan [9], Broutman and Kobayashi [10] and Johnson and Radon [11]. The results of these tests explain the relative scatter between the data given by the early experiments where only one parameter was systematically varied, and the other allowed to float. Marshall and Williams [12] provide a useful correlation of crack speed and crack resistance from the work of numerous authors. During the refereeing of this paper, two other papers appeared in this journal [37, 38], which relate to the cracking of PMMA. A brief discussion of some of the interesting points which are raised has now been incorporated into Section 4.

In broadest terms, all the data show that during stable crack propagation the resistance to cracking in PMMA increases as the crack velocity increases, and as the temperature decreases (n.b. this is contrary to the usual behaviour of toughness in metals). Explanations for the crack resistance behaviour have been put forward in terms of various molecular relaxation processes, e.g. Boyer [13]. Fluctuations in the foregoing time/temperature/toughness trends have been identified with damping peaks by Johnson and Radon [11], and time-temperature transformations of data have been performed by Olear and Erdogan [9] and Broutman and Kobayashi [10]. The associated activation

energies give some guidance for the particular molecular processes thought to occur in the cracking of PMMA. A discussion of these results is given later in this paper, along with the recent results of Lee [14].

There are various methods of characterizing resistance to cracking in materials. Some workers in the polymer field modify the classical Griffith analysis for fracture, and hence talk in terms of a fracture surface-free-energy (γ). Others appeal to "fracture mechanics" and use the concepts of a critical stress intensity factor (K_C) or critical strain energy release rate (G_C). Another method is to measure the specific work of fracture (i.e. fracture toughness, R) of a quasi-statically propagating crack. Conventional methods of obtaining the toughness of metals are complicated when applied to polymers, as the compliance calibrations vary with different cross-head velocities and different crack speeds during propagation because of rate-dependent moduli. Such difficulties compound the inherent uncertainties of slope measurement in rates of change of compliance determinations. Again, the appropriate Young's modulus for conversion between K and G is not always clear in polymers because of rate effects. Gurney and Hunt's sector area method for R [15] is a powerful tool in these circumstances, and it eliminates all tedious compliance calibrations. Moreover, the method yields many incremental toughness values from one test; these may often reflect rate dependency in the work of fracture if the testpiece is designed such that the crack velocity varies during quasi-static propagation. This should be contrasted with the "one-off" crack initiation values for K or G usually obtained from fracture mechanics techniques.

The work reported in this paper was aimed at determining relationships between the fracture toughness of PMMA obtained at different temperatures and crack speeds. Toughness was measured by Gurney and Hunt's method during propagation and, additionally, initiation K_C values were determined. A single type of test specimen of "compact tension" profile was used throughout for several reasons. Briefly, it allows good control of crack path without recourse to grooving; changes in cross-head velocity produce proportional changes in crack velocity, so that rate processes at the crack tip are proportional to the cross-head speed and crack length. The crack velocity (at constant cross-head velocity) slows down almost by a decade in one test; with a fixed starting crack length, a uniform specimen for measurement of the stress intensity factor is provided over all ranges of temperature and rate. The testpiece possesses good stability characteristics which means that occasional fast initiation fractures, caused by badly prepared blunt cracks, do not completely ruin the experiments and allow valid toughness data to be obtained during the subsequent propagation.

2. Experimental procedure

Specimens of commercial grade "Plexiglas G" were machined to the geometry shown in Fig. 1. The milled crack starter slots were fatigued in an Instron testing machine to a length of $\sim$ 51 mm.

The monotonically loaded cracking experiments to measure toughness were performed using cross-head speeds between 833 nm sec^{-1} and 8.33 mm sec^{-1}. Temperatures were varied between 193 and 353 K in an "environmental chamber" supplied for use with the testing machine; the actual temperatures of the specimens were measured with a copper–constantan thermocouple. The displacement of the loading pins was sensed by an extensometer adapted to a

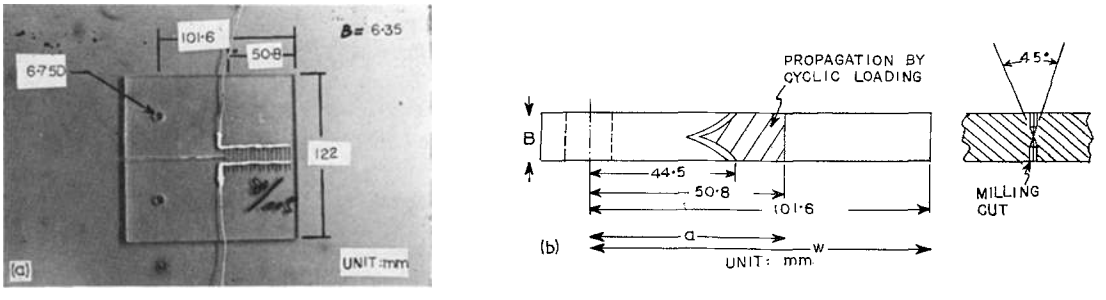

Figure 1 Geometry of the "compact tension" profile testpiece used for all experiments. Painted circuits in path of crack employed only at high crack velocities. (a) Fracture specimen; (b) specimen preparation.

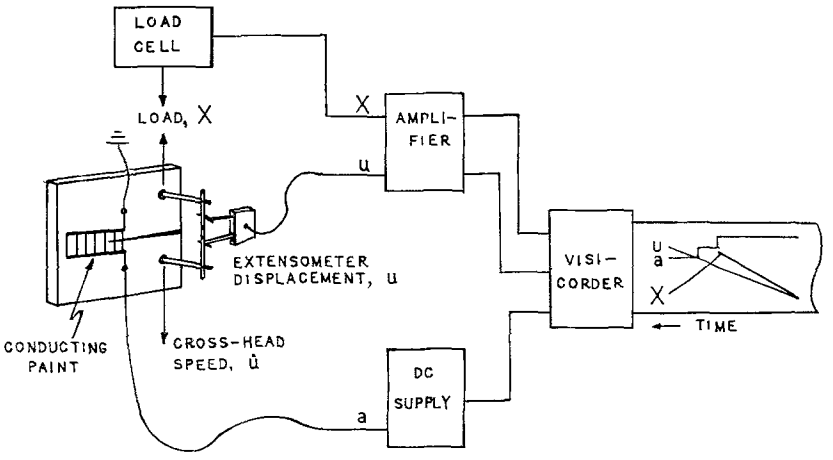

Figure 2 Arrangement of Visicorder circuitry to record crack load, crack length, and specimen opening displacement.

sliding pin assembly; this is similar to the clip-on gauge arrangements recommended by ASTM [16].

Crack propagation could be monitored visually during many tests, in which case the clip-on extensometer was made to drive the testing machine chart paper, and the position of the crack front was "pipped" on to the load/displacement trace. Load/displacement/crack length information was thus available directly from the chart paper, free of the effects of testing machine stiffness.

When the crack velocity exceeded 1 or 2 mm sec^{-1}, visual tracking was inaccurate. Specimens which had painted electrical resistance circuits in the path of the crack were then used. In these experiments, signals from the testing machine load cell, the clip-on extensometer and the resistance paint circuit were all fed into separate channels of a Honeywell 906C "Visicorder". Fig. 2 depicts the arrangement. Crack speed was obtained directly from the chart of the Visicorder, and the corresponding load/displacement/crack length curves were reconstructed from the chart output.

An oscilloscope was used to record "fast" data on occasion at those crack speeds which were beyond the response time capability of the Visicorder. Crack speeds up to 230 m sec^{-1} were produced at room temperature by the fastest available Instron cross-head speed. It was noted that the load appeared to remain constant while the crack propagated, and then to fall off out of phase with the crack movement. This suggests inertia effects; in such cases no attempt was made to determine toughness values. Some comments on kinetic effects and the validity of data taken when crack velocities are very high are made later in this paper.

3. Results

Fig. 3 shows a typical Visicorder record of load,

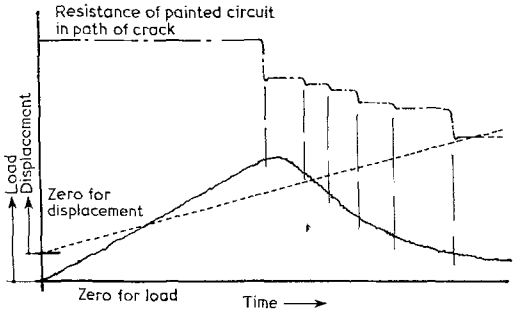

Figure 3 Typical Visicorder record of load, displacement and crack length.

P, displacement, u, and crack length, a, as the chart moves at a constant speed. This information is replotted as a load/displacement graph shown in Fig. 4, where each sector area corresponds to 6.35 mm crack propagation (i.e. about 40 mm^2 increase in crack area). Graphical measurement, by means of a planimeter, led to the toughness values shown. Load/displacement plots similar to Fig. 4 were obtained directly from the Instron chart paper when the cracks were monitored visually. The crack speed ($\dot{a}$) slows down significantly as the crack propagates in the particular testpiece used. Consequently,

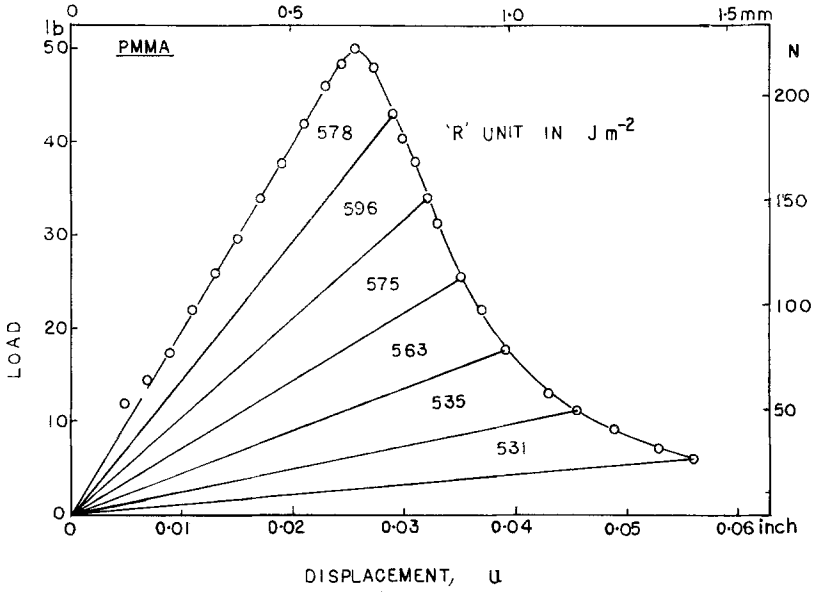

Figure 4 Information of the type shown in Fig. 3 plotted as load/displacement graph. Every sector area corresponds with about 6.35 mm crack propagation (i.e. $\sim$ 40 mm^2 increase in crack area). Similar load/displacement plots are obtained directly from the testing machine when the crack position is monitored visually.

rate-dependent R values will vary from those measured at the starting region to those measured at the end of the specimen. Thus, as explained in Section 1, a range of $R(\dot{a})$ values are obtained from one testpiece at every test temperature. Changes in the range of $\dot{a}$ may be obtained by changing the cross-head velocity, $\dot{u}$; checks on the $R(\dot{a})$ data can be performed by making the ranges of $\dot{a}$ overlap, i.e. the R values obtained early in a "slow" test can correspond with those measured at the end of a "fast" test.

Stress intensity factors for crack initiation (K_C) were obtained for every load/displacement curve, using the peak crack initiation load in the Gross-Srawley expression for the compact tension testpiece, e.g. ASTM [16] namely $K_C BW^{1/2}/P = f(a/w)$, see Fig. 1. Independent confirmation of the $f(a/w)$ function for PMMA specimens was obtained by compliance calibrations taking into account the effects of rate and temperature on the modulus. In our compact tension cracking experiments, there was hardly any deviation from linearity or "rounding" in the P versus u plots before the crack started to propagate continuously; hence the use of the maximum in the P versus u curve for K_C. It would appear from [37] that there also was essentially no "sub-critical" cracking in Outwater double torsion specimens or in tapered double cantilever beam testpieces. The slow crack growth under increasing load in the single edge notch specimens reported by Marshall *et al.* [37] seems peculiar to that type of specimen, for reasons that are investigated in the discussion of this paper.

Fig. 5a and b are semi-logarithmic plots of the experimental data of R as a function of crack speed for various temperatures. Fig. 6 shows the derived K_C values for crack initiation as a function of temperature for various cross-head speeds. Most of these data were obtained from experiments in which cracking was stable. The lowest crack speeds correspond with the slowest cross-head speed available (833 nm sec^{-1}). R values tend to level off to about 250 to 300 J m^{-2} at the low end of the crack speed range for every temperature. This seems to agree with the findings of Marshall *et al.* [17] who suggest that there exists a lower limit of toughness, (given in terms of K_{IC} in their case) below which no significant crack extension is observed.* An upper limit of crack speed was reached in the

*At the highest temperature used in our experiments (353 K), the slowest cross-head speed produced a plastic zone around the crack front with no crack propagation. Severe crazing, especially at 45° to the initial crack direction was seen. This behaviour is typical of high toughness/low strength polymers, such as polycarbonate at room temperature. Higher cross-head speeds and lower temperatures suppress the plastic zone in PMMA.

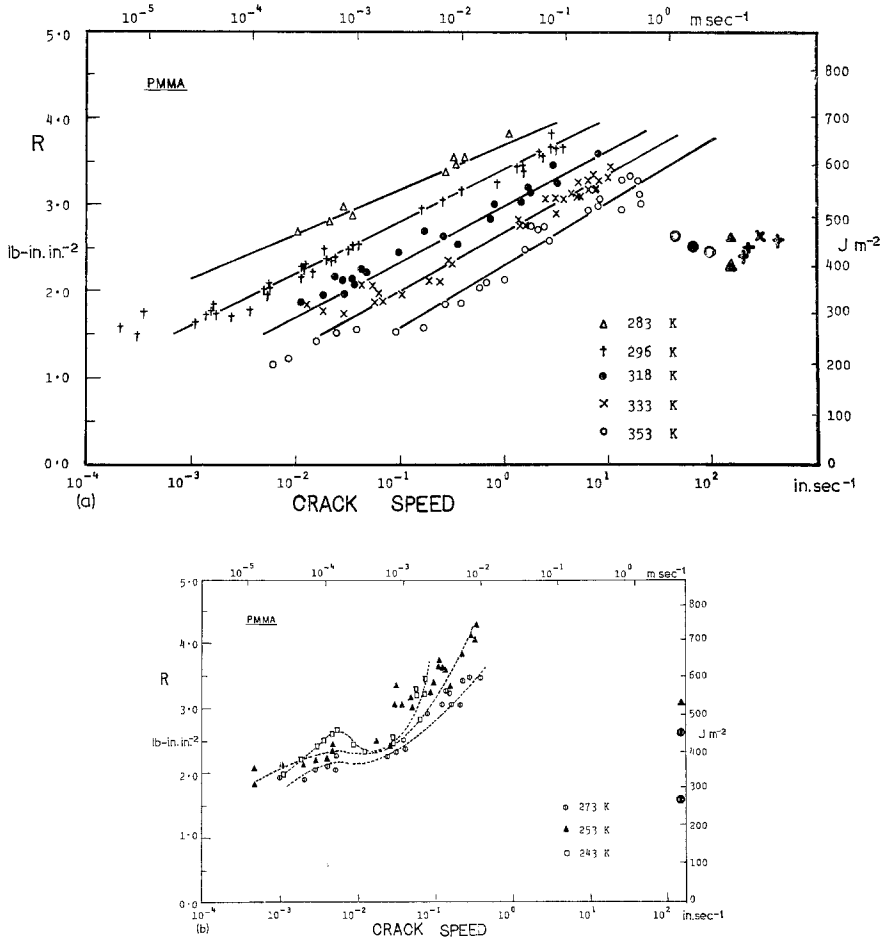

Figure 5 Experimental values of fracture toughness plotted against crack speed, (a) for temperatures of 283 K and greater, (b) for temperatures at 273 K and lower.

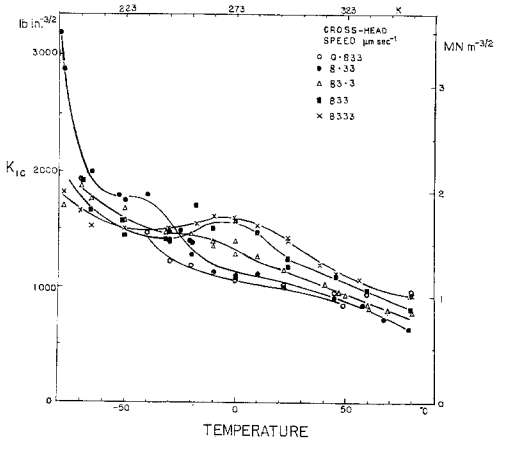

Figure 6 K_C data plotted against temperature for various cross-head speeds.

experiments, beyond which stable cracking was impossible. The upper limiting velocity varied with temperature, being about 600 mm sec^{-1} at 353 K and decreasing with temperature to about 2 mm sec^{-1} at 243 K. The range of stable crack propagation velocities thus diminished as the temperature fell, and at 233 K *no* stable crack growth was possible, even at the very low cross-head speed of 833 nm sec^{-1}. K_C determinations were possible of course right down to the lowest available temperature (193 K).

In the unstable range, upper bound estimates for R were obtained by taking the complete triangular area below the loading line and dividing by the testpiece cracked area. Approximate estimates were available for the corresponding crack speeds. It is significant that these R values plotted at the right hand side of Fig. 5a

and b, even though upper bounds, are all *lower* than the final stable R values obtained at the same temperatures. This is relevant to the causes of instability and is discussed in more detail in Section 4.3.

4. Discussion

4.1. Comparison with other data

In general terms, the toughness values given in Figs. 5 and 6 agree with those of other workers referenced earlier in this paper where measured in similar ranges of temperature and crack speed. Comparison with Johnson and Radon's K_C initiation data [11] is not quite so straight forward because $\dot{K}$ (the rate of change of stress intensity factor during load application) differs between the various types of test specimen, and in Johnson and Radon's case they used a variety of testpieces, namely, single edge notch tensile specimens, double cantilever beam cleavage testpieces and three-point bending "low blow" instrumented impact specimens. Nevertheless, the agreement between their results and those here is not unreasonable.

Fig. 6 shows a consistent increase in K_{IC} as the temperature decreases from 353 to 283 K for all the cross-head speeds involved. The highest K_C values are produced by the highest cross-head velocities, i.e. $dK_C/d\dot{u}$ is positive. As the temperature decreased further below 283 K some transitional behaviour was displayed. For example, at the highest cross-head speed a maximum occurs at about 273 K. Similar peaks are shown at lower temperatures for lower cross-head speeds, and below about 240 K the highest K_C values are produced by the slowest cross-head speeds (i.e. below 240 K $dK_C/d\dot{u}$ is negative). At the lowest temperature available on our apparatus (193 K) there is evidence of another possible set of maxima. Although, again, direct comparison with the results of Johnson and Radon is not possible, the peaks in Fig. 6 are similar to their observations. The fracture toughness, R, data obtained from continuous crack propagation also display peaks and inversions, over similar ranges of temperature as shown in Fig. 5 and in the unstable range yield *low* upper bound values.

4.2. Toughness mechanisms and activation energies

Boyer, in his review article [13], observed that secondary relaxation mechanisms may provide the molecular motion for the plastic flow of polymers below the glass transition range. He suggested that stable crack growth may be an extension of craze growth at the tip of an advancing crack which, in turn, is governed by β secondary relaxation mechanisms (see also Kambour [18]; Doyle *et al.* [19]). An attempt by Heijboer [20] to correlate impact tests with 1 kHz dynamic mechanical measurements was not successful. However, Johnson and Radon [11] have identified peaks in K_{IC} curves (similar to Fig. 6) with dynamic damping peaks. They assumed that the "time to fracture" in their toughness tests was equivalent to the period used in the independent "tan δ" damping loss measurements. Using cross-head speed as a rate parameter in an Arrhenius equation, Johnson and Radon calculated an activation energy of 24 kcal mol^{-1} ($\sim$ 100 kJ mol^{-1}) from their K_{IC} results.*

Although there have been many studies on the kinetics of craze growth in PMMA (e.g. Sauer and Hsiao [22]; Regel [23]; Higuchi [24]), the total physical range of craze growth was usually less than 1 mm. There seem to have been few studies on craze growth in glassy polymers during *continuous* crack propagation – for example, Marshall *et al.* [17] studied PMMA crack growth rates in an environment of methanol in terms of an initiation K and not some current K during propagation. Zhurkov [25] made a general study of the kinetics of the fracture of solids under dead load conditions and found that a wide range of materials followed a *stress-biased* Ree-Eyring failure kinetics relationship of the sort,

$$t_f = A_0 \exp\left(\frac{U - \phi\sigma}{kT}\right) \quad (1)$$

where t_f is the time to failure measured from the moment of loading, and where T is absolute temperature, k is Boltzmann's constant, A_0 and ϕ are constants, U is the activation energy and σ is the applied stress. Equation 1 was applied to uniaxial specimens of small diameter for which the fracture propagation time was negligible compared to the crack initiation time.

It may be plausible to argue that crack speed is inversely proportional to the fracture time of molecules, and that the stress at the crack tip is proportional to fracture toughness by a relation-

*Olear and Erdogan [9] were able to superimpose K_{IC} versus temperature data for PMMA using a shift function that was identical to the *relaxation modulus* shift function reported by McLaughlin and Tobolsky [21].

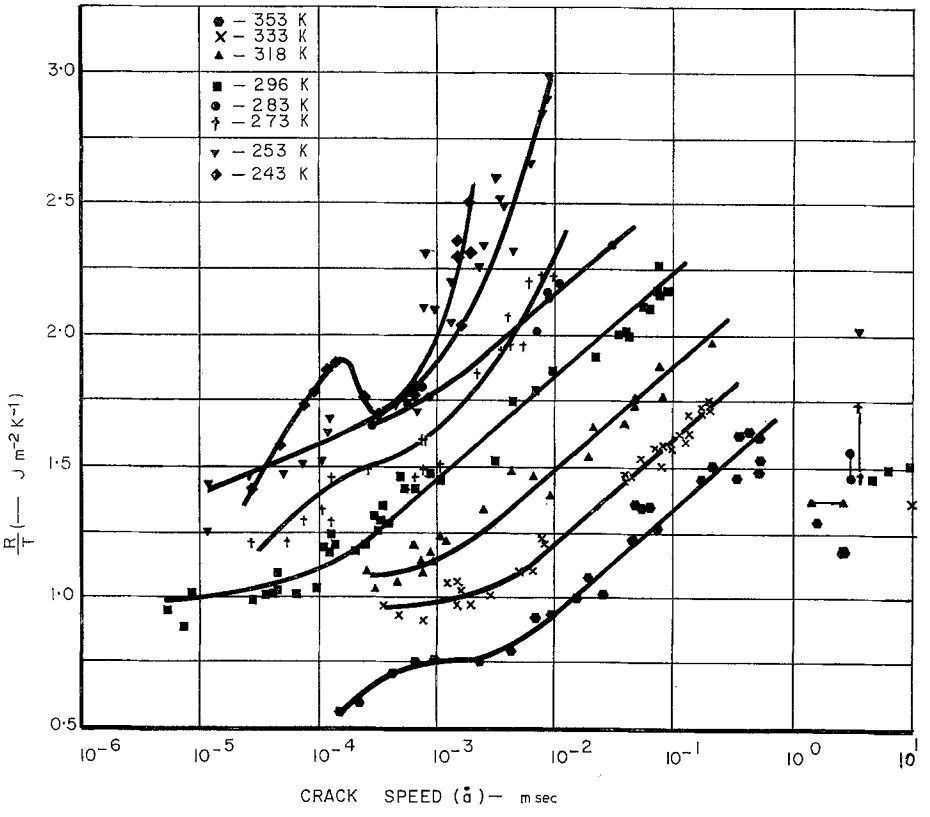

Figure 7 R/T versus crack velocity at various temperatures.

ship such as $\sigma = R/u_c$, where σ is the stress state in the crazed material near the crack tip and u_c is the displacement at the crack tip. If so, one might wonder whether the fracture toughness of PMMA could be represented by a *toughness-biased* Ree-Eyring expression such as

$$\dot{a} = A_1 \exp\left(\frac{-[U - \lambda R]}{kT}\right) \qquad (2)$$

where $\dot{a}$ is the crack velocity during continuous propagation, R is the fracture toughness (equivalent to the strain energy release rate, G) and A_1 and λ are constants. This type of equation has been used for glass by Schönert *et al.* [26] and Kies and Clark [27].

Since Equation 2 may be written

$$\frac{R}{T} = \frac{k}{\lambda} \ln \frac{\dot{a}}{A_1} + \frac{U}{\lambda T} \qquad (3)$$

it suggests that the R versus $\dot{a}$ data of Fig. 5 should be replotted as R/T versus $\dot{a}$. Fig. 7 shows the result. The parallel lines at constant temperature predicted by Equation 3 are satisfied reasonably well in the higher crack speed and higher temperature ranges (right hand side of diagram). In the temperature range 283 to 353 K, the activation energy obtained from Equation 3 is about 86 kJ mol^{-1} (21 kcal mol^{-1}). This value, and that given by Johnson and Radon [11], support Boyer's contention that stable cracking is craze growth, governed by the secondary β-process.*

$\lambda = 53.4$ m^2 mol^{-1} $= 8.9 \times 10^{-23}$ m^2 using Avagadro's number. Kies and Clark [27] suggest that $\lambda = \beta d_o^2$ where β is the fraction of the toughness work actually used in breaking bonds, and d_o is the bond spacing, which, in the present

*Broutman and Kobayashi [10] horizontally shifted their G versus $\dot{a}$ data, but as the slopes are evidently not constant (Fig. 5) a range of activation energies would be obtained. They quoted two values, namely, ~ 9 kcal mol^{-1} (39 kJ mol^{-1}) for crack velocities less than 65 mm sec^{-1} and 34 kcal mol^{-1} (143 kJ mol^{-1}) for higher velocities, which led them to suggest that a primary (α) relaxation mechanism controls fracturing at low velocities, and a secondary (β) mechanism at high velocities. This seems at odds with all other published work. A simple Arrhenius treatment (i.e. Equation 2 without the R term) of our R data (which essentially agree in value with those of Broutman and Kobayashi), gives an activation energy in the range 283 to 353 K of some 66 kJ mol^{-1} (15.5 kcal mol^{-1}).

context, is presumably the inter-chain spacing. If the latter is about 0.7 nm in PMMA, $\beta = 1.8 \times 10^{-4}$, so that with R about 500 J m^{-2}, $\beta R = 0.1$ J m^{-2}. If instead we use $d_o = 0.15$ nm as the carbon–carbon bond distance, $\beta = 4 \times 10^{-3}$ and $\beta R = 2$ J m^{-2}. Both βR values are of the order of magnitude of the surface free energy of PMMA, the rest of R going into craze formation. It would appear that the 0.7 nm spacing result suggests that it is Van der waals bonding forces that are being broken, rather than carbon–carbon bonds.

Crack resistance versus crack speed data below 283 K do not follow the same family of curves predicted by Equation 3. The change in the propagation fracture toughness behaviour seems to be consistent (at least qualitatively) with the crack initiation K_{IC} results shown in Fig. 6. K_{IC} values for all cross-head speeds (over four decades) show a steady increase as the temperature decreases until 273 K when the K_{IC} at the highest cross-head speed (8.33 mm sec^{-1}) reached a maximum. It is at about this same temperature that the R versus $\dot{a}$ curve starts to deviate from the family of curves predicted by Equation 3. At lower temperatures, the K_{IC} curves corresponding to slower cross-head speeds reach either maxima or plateaux. It seems likely that the behaviour may be related to a transition of the molecular relaxation mechanisms involved in the fracture process.

It was mentioned earlier that Johnson and Radon [11] applied time-temperature relationships of the Boltzmann type to K_C data. We have attempted to derive complementary activation energies from Fig. 6, from the simple equation

$$\dot{u} = A \exp\left(\frac{-U}{kT}\right). \tag{4}$$

However, a wide range of activation energies can be obtained, depending on the constant K_C value chosen from which $K(\dot{u}, T)$ data are taken. For example, a value for U (82 kJ mol^{-1}) very close to that obtained from the R data (86 kJ mol^{-1}) fits the $\dot{u}$ versus $1/T$ data taken at $K_C = 1.5$ MN m$^{-3/2}$; however, at $K_C = 1.0$ MN m$^{-3/2}$, U is 172 kJ mol^{-1}.

Given the reasonable success of Equation 2 in portraying the $R(\dot{a}, T)$, we should not expect Equation 4 to apply (cf. the method of Broutman and Kobayashi [10] for determining U). Writing K^2/E for R in Equation 2, we have

$$\dot{a} = A_1 \exp\left(\frac{-[U - \lambda K^2/E]}{kT}\right) \tag{5}$$

so that transformations of K^2/ET versus $\dot{u}$ might be successful, (for those cases where $\dot{a} \propto \dot{u}$) but not transformations of K alone. Unfortunately, E is rate and temperature dependent, and the crack tip strain rate that gives the appropriate E is not always obvious. Williams [28], however, has argued that K_C for PMMA can be described in terms of a fixed crack opening displacement (cod) and yield strain (e_y), in which case K_C^2/ET becomes

$$\frac{K(\text{cod})^{1/2}(e_y)^{1/2}}{T}.$$

Then

$$K_C/T = \frac{k}{\lambda(\text{cod})^{1/2}(e_y)^{1/2}} \ln \frac{\dot{u}}{CA} + \frac{U}{\lambda(\text{cod})^{1/2}(e_y)^{1/2}T} \tag{6}$$

where $\dot{a} = \dot{u}/C$. The semilogarithmic plot (not shown here) suggested by Equation 6 is not as successful in describing the K_C data of Fig. 6, as Equation 2 does the R data of Fig. 5a. There is a consistent reduction in slope as T increases, although with $(\text{cod})^{1/2} e_y^{1/2} \approx 10^{-3}$, the slope ($\sim 155$) suggested by Equation 6 is not too bad. However, there is some arbitrariness in determining U, values of which are about twice the value obtained from Equation 3.

4.3. Crack instability and crack tip temperatures

Crack stability means different things to different people. Our understanding of stability in cracking follows the ideas put forward by Gurney and his co-workers [e.g. 15, 31]. Stability must be defined relative to some chosen constraints, such as the stiffness of the testing machine. In a hard testing machine $du > 0$; in a soft machine $dP > 0$. Imposing such constraints onto the basic energy rate balance for cracking, i.e. to changes in external work, internal work (strain energy) and toughness work, the condition for stability in a hard machine may be written

$$\frac{1}{R} \cdot \frac{dR}{dA} \leqslant \text{(g.s.f)}, \tag{7}$$

$$\text{i.e. } \frac{1}{R}\left(\frac{dR}{d\dot{a}}\right)\left(\frac{\ddot{a}}{B\dot{a}}\right) \leqslant \text{(g.s.f)}.$$

$(1/R)(dR/dA) = (1/R)(dR/d\dot{a})(\ddot{a}/B\dot{a})$ concerns

rate effects in the toughness, where $\dot{A}$ is the crack areal velocity, $\dot{a}$ the crack linear velocity, $\ddot{a}$ the crack acceleration and B is the specimen thickness.

The geometric stability factor (g.s.f.) of the specimen under consideration is given by

$$(\text{g.s.f}) = \frac{(\mathrm{d}^2/\mathrm{d}A^2)\,(P/u)}{(\mathrm{d}/\mathrm{d}A)\,(P/u)} = \frac{(\mathrm{d}^2/\mathrm{d}A^2)\,(u/P)}{(\mathrm{d}/\mathrm{d}A)\,(u/P)} - \frac{2(\mathrm{d}/\mathrm{d}A)\,(u/P)}{(u/P)}. \quad (8)$$

The various rates of change of compliance can be deduced from fracture mechanics expressions for the particular testpiece, or by other means, to give the specimen g.s.f.

Physically, the circumstances surrounding an unstable crack are such that, as the crack starts to propagate, there happens to be so much strain energy present at crack initiation that the system could afford to return work from the specimen to the loading machine, and still have enough energy left to satisfy the work of fracture requirements during propagation. As typical testing machine cross-heads do not reverse in a test, the excess energy is dumped into the specimen, leading to an accelerating unstable crack. Note that there are two factors which determine stability, namely, the g.s.f. which is a function of specimen and loading mode, and the factor which depends on rate and possibly temperature effects in the material being investigated.

Large negative g.s.f. values favour stability, because if R is constant, $\mathrm{d}R/\mathrm{d}A = 0$, and $0 >$ (negative number). Specimen geometries which are known to be unstable with constant R values (such as the Griffith case or the SEN specimen used by Marshall *et al.* [37]) have positive g.s.f.'s, so that stable cracking is impossible unless $\mathrm{d}R/\mathrm{d}A$ or $\mathrm{d}R/\mathrm{d}\dot{a}$ is sufficiently positive – which happens for PMMA – (i.e. when it requires increasing amounts of work to propagate the crack at higher velocities).

The g.s.f.'s of two testpieces that produce stable cracks with R constant are:
compact tension (used here),

$$\text{g.s.f} = -\frac{8.6}{BW}\left(\text{for } \frac{a}{w} = 0.5\right)$$

and Outwater double torsion (used in [37]),

$$\text{g.s.f} = -\frac{2}{Ba}\left(= -\frac{4}{BW} \text{ for } \frac{a}{w} = 0.5\right)$$

where B is specimen thickness, W the length of the specimen in the path of the crack, and a is the crack length. Unstable cracks can be produced in these inherently stable testpieces, of course, if $\mathrm{d}R/\mathrm{d}\dot{a}$ becomes sufficiently negative for some materials. Note that the "more stable" compact tension testpiece may be made "less stable" than the Outwater specimen by choice of dimensions. Grooving the Outwater specimen for example, reduces B in the path of the crack so that

$$\left|-\frac{2}{Ba}\right| > \left|\frac{-8.6}{BW}\right|.$$

None of our specimens was grooved, unlike the Outwater specimens in [37]; the complete dimensions of the double torsion testpieces are not given in [37] for a check to be made, but it would seem that a more negative g.s.f. (i.e. grooving and $a < 0.5W$) allowed Marshall *et al.* [37] to obtain stable Outwater cracking down to temperatures of 213 K, whereas we were unable to produce stable cracks in our compact tension specimens below 243 K.

The right hand "end" data points in Figs. 5 and 7 give the crack speeds at which unstable cracking was observed in our experiments. There is a gradual reduction in the unstable velocities with decreasing temperature; below 243 K no stable cracking was attainable, even at the slowest available cross-head velocity (833 nm sec^{-1}). The sudden change to unstable behaviour has been explained in terms of (i) a molecular relaxation transition (i.e. tan δ peak) by Johnson and Radon [11], (ii) an isothermal to adiabatic transition at the crack tip which causes local softening and reduction in toughness (e.g. [28]) and, recently, (iii) a transition in craze formation ahead of the crack tip from merely one plane at low velocities to many planes at high velocities (with an associated energy-absorbing shear mechanism that coalesces the crazes) which causes a discontinuity in toughness [29].

Williams and Marshall [30] have presented results which tend to favour the isothermal-adiabatic mechanism over the tan δ peak mechanism. The temperature build-up in a crack tip Dugdale zone was analysed and incorporated into an expression for K_C. Using $\mathrm{d}K_C/\mathrm{d}\dot{a} = 0$ as the condition for instability, critical crack speeds were obtained for the ambient temperature of every test. Excellent agreement was found with their experimental data determined from Outwater plate bending (double torsion) specimens, Fig. 8.

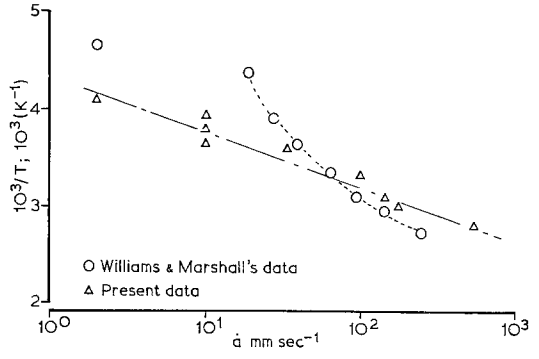

Figure 8 Limiting experimental unstable crack velocities plotted against the reciprocal of temperature.

Our own results for the critical crack speeds are also shown in Fig. 8; in general terms there is agreement, but our data vary more gradually with $1/T$. An attempt was made to predict the critical speed, along the lines of Williams and Marshall [30] assuming that Equation 3 could be applied to the locally heated crack tip zone. In the present analysis, we have used the Gurney condition of instability (i.e. Equation 7), rather than merely $dK_C/d\dot{a} = 0$ or $dR/d\dot{a} = 0$. That these latter conditions cannot be sufficient criteria for unstable fracture is realized when we note that there are local maxima and minima in $(R, \dot{a})$ and $(K_C, \dot{a})$ relationships where the cracking is known to be stable, for example at low velocities and high temperatures in Figs. 5 and 6. Evidently there are conditions where the left hand side of Equation 7 does not satisfy the inequality, even when $dR/d\dot{a}$ is slightly negative.

For the critical velocity analysis, we have from Equation 3

$$\frac{dR}{d\dot{a}} = \frac{Tk}{\lambda\dot{a}} + \ln\left(\frac{\dot{a}}{A}\right) \cdot \frac{k}{\lambda} \cdot \frac{dT}{d\dot{a}} \cdot \tag{9}$$

With no adiabatic heating, $dT/d\dot{a} = 0$ and $dR/d\dot{a}$ is always positive,which clearly promotes stability. From the simplified adiabatic temperature rise for the crack tip zone, i.e.

$$(T - T_0) = \frac{R}{\rho c b} \tag{10}$$

(where T_0 is the ambient test temperature, ρ the density, c the specific heat, and b the thickness of the plastic zone), we have

$$\frac{dT}{d\dot{a}} = \frac{Tk}{\lambda\dot{a} - (k\dot{a}/\rho c b)\ln(\dot{a}/A)} \tag{11}$$

Whence, at the crack tip instability, $dR/d\dot{a} = (BR)$ (g.s.f)$/(\ddot{a}/\dot{a})$ or

$$\frac{Tk}{\lambda\dot{a}} + \ln\frac{\dot{a}}{A} \cdot \frac{k}{\lambda} \cdot \left[\frac{Tk}{\lambda\dot{a} - (k\dot{a}/\rho c b)\ln(\dot{a}/A)}\right] = \frac{(-13.3 \times 10^3)}{(\ddot{a}/\dot{a})} B\left[\frac{Tk}{\lambda}\ln\frac{\dot{a}}{A} + \frac{U}{\lambda}\right] \tag{12}$$

which, with the values for λ, k, A deduced earlier, and $\rho = 1.2 \times 10^3$ kg m^{-3}, $c = 1.5 \times 10^3$ J kg^{-1} K^{-1} $b \approx 10^{-4}$ m, becomes

$$T/\dot{a} + (\ln\dot{a} - 18.4) \cdot \left[\frac{0.155T}{\dot{a}\{1 - 8.64 \times 10^{-4}(\ln\dot{a} - 18.4)\}}\right] = \frac{-84.5}{(\ddot{a}/\dot{a})}\left[1.04 \times 10^4 + T(\ln\dot{a} - 18.4)\right]. \tag{13}$$

Clearly this cannot be solved without knowledge of the crack acceleration at instability ($\ddot{a}$), which we do not know. However, the general trend of Equation 13 is that the critical crack velocity decreases with temperature in accord with the experiments. The accelerations that make Equation 13 agree with the experimental $(\dot{a}, T)$ combinations diminish gradually with decreasing temperature, from about 170 m sec^{-2} at 353 K, through 5 m sec^{-2} at 296 K, to $\sim 2 \times 10^{-3}$ m sec^{-2} at 243 K, (although it must be remembered that Equation 3, which has been used in the derivation of Equation 13, does not hold below about 283 K.) Nevertheless, a diminishing $\ddot{a}$ at instability helps the inequality of Equation 7. Moreover as T diminishes, $dR/d\dot{a}$ from Equation 9 gets more negative because of the $dT/d\dot{a}$ adiabatic heating term. Both factors tend towards unstable fracture, and although we have no $R(T, \dot{a})$ data for $T < 243$ K, we note that the K_C curves "flip flop" at about 230 to 240 K, and at lower temperatures $dK_C/d\dot{a}$ is negative (Fig. 6). Thus our inability to produce stable fractures at these low temperatures in compact tension specimens seems to be associated with negative $dR/d\dot{a}$ gradients that fail to satisfy the stability inequality in Equation 7 for the particular g.s.f. value of the size of our specimens. The same may be said about the unstable fractures we saw at high velocities and high temperatures. As *upperbound* R values were less than the final stable R values, $dR/d\dot{a}$ must be negative.

The difference in curves between the critical crack speeds and reciprocal of temperature for the Outwater data presented by Marshall *et al.* [30, 37] and the present data are interesting. As

mentioned previously, the Outwater specimen may be made geometrically more stable than the compact tension specimen, caeteris paribus, by side grooving. In principle, more stable specimens should withstand higher instability temperatures for the same $\dot{a}$, i.e. the $1/T$ versus $\dot{a}$ slope should be lower the more stable the specimen. It would be interesting to know the precise g.s.f. of the Outwater specimens used in [37]; in particular, we wonder whether *deeper* side grooving was employed on the testpieces used at the lowest temperatures ($\sim$ 213 K). Such grooving would promote stability, and would perhaps explain why that one experimental result at 213 K does not seem to fit the rest of the Outwater data.

The crack tip temperature increases associated with the adiabatic heating are quite modest from the calculations of Williams and Marshall [30], namely, 10 K at a testing temperature of 213 K (when $\dot{a} \sim 1$ mm sec^{-1}), and 30 K at 353 K ($\dot{a} \sim 240$ mm sec^{-1}). Fox and Fuller [33], using an infra-red detector, determined that the crack tip temperature rise was about 450 K at room temperature when a crack in PMMA was travelling at the much faster velocity of $\sim$ 580 m sec^{-1}. Recent calculations by Weichert and Schönert [34], for glass, predict local rises of over 1000 K for velocities of 1000 m sec^{-1}. In the case of PMMA at high velocities, the toughness measured at room temperature increases rapidly around 100 m sec^{-1} – Broutman and Kobayashi [10] measuring values for R of 1000 J m^{-2}, and Green and Pratt [29] determining K_C values of over 10 MN m$^{-3/2}$. Although doubt may be cast on these precise values for toughness, since in none of the analyses were kinetic energy effects taken into account, (for an account of which see Gurney and Ngan [35]), nevertheless the increased energy dissipation produced by multiplane crazing must promote high crack tip temperatures.

It seems to us that the isothermal/adiabatic mechanism proposed by Williams [28] explains the crack instabilities that we have observed in our lower speed experiments, rather than the Green and Pratt multiplane crazing mechanism. One piece of evidence to support this contention concerns crack surface fractography, distinct changes in which were observed in the experiments. Details are presented in Part 2 of this paper [36]. At very slow crack velocities, the surfaces were featureless to the naked eye, but became increasingly rougher at higher velocities. At the unstable velocities to which the isothermal/adiabatic model is supposed to relate, the surfaces again became smooth (displaying conical markings under the microscope). Smooth, apparently featureless, surfaces were characteristic of all the unstable K_C experiments between 193 and 243 K, and of those experiments at higher temperatures where the crack velocities were a little greater than the isothermal/adiabatic critical values. We did not see the rough surfaces of multiplane crazing. However, at the higher crack velocities (say, > 3 m sec^{-1}) where "quasi-stable" crack propagation, consisting of a series of small arrested jumps, was observed by Broutman and Kobayashi [10] and Green and Pratt [29], it would appear that multiplane crazing re-introduces a measure of crack stability during propagation.

4.4. Slow crack growth in "unstable" specimens

The g.s.f. of the SEN specimen tends towards instability, so that for constant R, all tests would be expected to go "bang". Since, however, slow crack growth under rising load is observed in PMMA SEN testpieces over a range of starting (a/W), it follows from Section 4.3 that $[1/R\,(\mathrm{d}R/\mathrm{d}\dot{a})]$ must be positive enough to promote stability according to Equation 7 in the region of slow growth. The system reverts to its inherent instability when $\mathrm{d}R/\mathrm{d}\dot{a}$ is reduced, and eventually made negative, by adiabatic heating as for the other testpieces discussed in Section 4.3. It should be possible to show mathematically why stability is achieved in the SEN specimen, and indeed the velocity and K_C value at which it then becomes unstable from knowledge of the $R(\dot{a}/T)$ behaviour; but the problem is rather messy at first sight.

Mai, who has also observed slow crack growth under rising load in SEN PMMA specimens reports [32] that, in his experience, the slow growth occurs only for $(a/W) < 0.25$ (but presumably not for very small (a/W) since ordinary unnotched tension bars do not seem to display slow growth). Unfortunately, the SEN specimen dimensions in [37] are not given, but the slow growth before fast fracture might be perhaps 10 mm from starting crack lengths of 10 to 20 mm in 76 mm wide SEN testpieces. Cracks start to move when the testing machine P versus u plot is still linear. Indeed, in Fig. 4 of [37] the initiation K_C values are about half the instability K_C values, so that if

$$K \propto P\sqrt{a}$$

$$\frac{dK}{K} = \frac{dP}{P} + \tfrac{1}{2}\frac{da}{a}$$

and if $dK/K = 1.0$ (i.e. K_C instability = 2 × K initiation) with

$$\tfrac{1}{2}\frac{da}{a} = 0.25 \text{ to } 0.5$$

(assumed 10 mm slow growth from 10 to 20 mm starter crack) then

$$\frac{dP}{P} = 0.5 \text{ to } 0.75$$

which means that initiation must be well down on the linear portion of the P/u plot, or that if sub-critical growth is to be identified with deviations from linearity, that the curvature in the P versus u plot must be rather subtle. Appreciable crack movement at observable velocities, however, does not seem to be observed with SEN specimens until there are obvious deviations from linearity in P versus u plots of usual u-axis magnification.

The K values from the Outwater and tapered DCB specimens quoted in [37] – with which our compact tension data essentially agree as functions of $\dot{a}$ and T – have been calculated from the steady propagation load and not from any lower "initiation" load on the P versus u plot which then blended over into the steady propagation load. As we have mentioned, "sub-critical" slow crack growth under rising load is absent in these specimens. Marshall *et al.* [37] have identified the toughness in the SEN slow growth region with the continuous propagation toughness of Outwater and tapered DCB testpieces at comparable crack velocities, where the slow growth velocity seems to be averaged over the time from crack initiation to crack instability. Since little observable movement can be observed until loads much closer to the maximum load in the P/u plot than the initiation load, Mai suggests [32] that better correlation would be obtained if some average SEN K, between initiation and instability in the SEN results, were to be used instead of the smaller initiation value. It seems significant that comparison of Figs. 4 and 8 in [37] shows that the SEN initiation data fall below the Outwater and tapered cleavage K values.

5. Conclusions

The fracture toughness of PMMA, over a certain range of temperatures and crack velocities, is well described by a toughness-biased Ree-Eyring relationship, the activation energy associated with which, suggests that cracking is controlled by craze growth and secondary (β) molecular processes.

However, the distinct change in fracture behaviour below 283 K means that the fracture behaviour cannot be characterized in terms of a single molecular relaxation mechanism for the whole temperature range of the present experiments.

Unstable cracking immediately outside the foregoing range of temperature and crack velocity seems to be produced by an isothermal-to-adiabatic transformation at the crack tip which causes local reductions in toughness; $dR/d\dot{a}$ is, therefore, made sufficiently negative to satisfy the instability condition for the particular testpiece used.

Acknowledgement

We wish to thank Dr Y. W. Mai for most helpful discussions of this paper.

References

1. J. J. BENBOW, *Proc. Phys. Soc.* (*London*) **78** (1961) 970.
2. N. L. SVENSSON, *ibid* 77 (1961) 876.
3. J. P. BERRY, *J. Polymer Sci.* **A1** (1963) 993; see also *J. Appl. Phys.* **34** (1963) 62.
4. L. J. BROUTMAN and F. J. MCGARRY, *J. Appl. Polymer Sci.* **9** (1965) 589.
5. P. L. KEY, Y. KATZ and E. R. PARKER, UCRL Report No. 17911, Berkeley, California (1968).
6. D. I. VINCENT and K. V. GOTHAM, *Nature* **210** (1966) 1254.
7. J. G. WILLIAMS, J. C. RADON and C. E. TURNER, *Polymer Eng. Sci.* **8** (1968) 130.
8. G. P. MARSHALL, L. P. CULVER and J. G. WILLIAMS, *Plastic and Polymers* **37** (127) (1969) 75.
9. P. D. OLEAR and F. ERDOGAN, *J. Appl. Polymer Sci.* **12** (1968) 2563.
10. L. J. BROUTMAN and T. KOBAYASHI, AMMRC Report CR 71-14, Army Mater. Mech. Res. Center, Watertown, Massachusetts, 1971; see also Proceedings of the International Conference on Dynamic Crack Propagation (Lehigh Univ.), edited by G. Sih, (Noordhoff, Groningen, 1973) p. 215.
11. F. A. JOHNSON and J. C. RADON, *Eng. Fract. Mech.* **4** (1972) 455.
12. G. P. MARSHALL and J. G. WILLIAMS, *J. Mater. Sci.* **8** (1973) 138.
13. R. F. BOYER, *Polymer Eng. Sci.* **8** (1968) 161.
14. C. S. LEE, Ph.D. Dissertation, University of Michigan (1974).
15. C. GURNEY and J. HUNT, *Proc. Roy. Soc.* (*London*) **A229** (1967) 508.

16. American Society for Testing and Materials, Special Tech. Pub. No. 463, 1970.
17. G. P. MARSHALL, L. E. CULVER and J. G. WILLIAMS, *Proc. Roy. Soc.* (*London*) **A319** (1970) 165.
18. R. P. KAMBOUR, General Electric Report No. 72 CRD 285, Schenectady, New York (1972).
19. M. J. DOYLE, A. MARANCI, E. OROWAN and S. T. STORK, *Proc. Roy. Soc.* (*London*) **A329** (1972) 137.
20. J. HEIJBOER, *J. Polymer Sci.* **C16** (1968) 3755.
21. J. R. MCLAUGHLIN and A. V. TOBOLSKY, *J. Colloid. Sci.* **7** (1962) 555.
22. J. A. SAUER and C. C. HSIAO, *ASME Trans.* **75** (1953) 895.
23. V. R. REGEL, *J. Tech. Phys.* (*USSR*) **26** (1956) 359.
24. M. HIGUCHI, Proceedings of the First International Conference on Fracture, Sendai, Japan, (1966) p. 1211.
25. S. N. ZHURKOV, *Int. J. Fract. Mech.* **1** (1965) 311.
26. K. SCHÖNERT, H. UMHAUER and W. KLEMM, Proceedings of the Second International Conference on Fracture, Brighton, England (1969) p. 474.
27. J. A. KIES and A. B. J. CLARK, Proceedings of the Second International Conference on Fracture, Brighton, England (1969) p. 483.
28. J. G. WILLIAMS, *Int. J. Fract. Mech.* **8** (4) (1972) 393.
29. A. K. GREEN and P. L. PRATT, *Eng. Fract. Mech.* **6** (1974) 71.
30. J. G. WILLIAMS and G. P. MARSHALL, *Polymer Letters* **15** (1974) 251.
31. C. GURNEY and Y. W. MAI, *Eng. Fract. Mech.* **4** (1972) 853.
32. Y. W. MAI, private communication.
33. P. G. FOX and K. N. G. FULLER, *Nature* **234** (1971) 13.
34. R. WEICHERT and K. SCHÖNERT, *J. Mech. Phys. Solids* **22** (1974) 127.
35. C. GURNEY and K. M. NGAN, *Proc. Roy. Soc.* (*London*) **A325** (1971) 207.
36. A. G. ATKINS, C. S. LEE and R. M. CADDELL, *J. Mater. Sci.* **10** (1975) 1394.
37. G. P. MARSHALL, L. H. COUTTS and J. G. WILLIAMS, *ibid* **9** (1974) 1409.
38. R. A. W. FRASER and I. M. WARD, *ibid* **9** (1974) 1624.

Received 21 October 1974 and accepted 13 January 1975.